DEVELOPMENT AND PERFORMANCE ANALYSIS OF A SINGLE AXIS LINEAR MOTOR TEST-BED

J. Moscrop, C. Cook and F. Naghdy

School of Electrical, Computer and Telecommunications Engineering
University of Wollongong, NSW 2522 Australia

Abstract

The ever-increasing demands placed on industrial machine tool manufacturers, for greater speeds and accuracies, are beginning to exceed the capabilities of current machine tool technologies. However, the ongoing revolution in computer, sensor and actuator technologies has introduced the potential of economically meeting these higher demands through new approaches in machine tool design. One actuator technology currently influencing high precision industrial automation is the linear motor. This paper details the development of a single axis linear motor test-bed, replicating one axis of a laser cutting machine tool. Through analysis of system stiffness and torque disturbances, the performance of the linear motor driven axis is compared to that of a more common ball screw driven axis.

1 INTRODUCTION

As tolerances on machined products are tightened, there is increasing pressure on industrial machine tool manufacturers to continually improve the accuracies of their machines. Since the push for higher accuracy is also often coupled with a push for higher response speed, these ever-increasing demands are beginning to exceed the capabilities of current machine tool technologies. However, as a result of emerging machine tool technologies in the computer, sensor and actuator areas, new approaches in machine tool design have introduced the potential of meeting these increasing demands. One example of an emerging machine tool technology is the linear motor. Although the very first linear motor was built in the early 1840's (by Wheatstone) [1], the use of linear motors in precision machine tools has only come under study relatively recently [2].

Traditionally, linear positioning in a machine tool axis is achieved through the use of a rotary motor and a mechanical transmission mechanism such as a ball screw. However, a number of known factors limit the accuracy of such linear positioning stages, including flexing of the mechanical transmission, friction, cogging, bearing vibration and backlash. As an alternative, a linear motor driven axis offers distinct advantages through elimination of the mechanical transmission mechanism. Such advantages include increased linear motion speed and dynamic response, the elimination of backlash, reduced friction and longer lifetime. However, elimination of mechanical structure also reduces system stiffness. As such, a linear motor driven axis is more sensitive to load variations and external disturbances (such as machining forces) [3, 4].

This paper describes the design and development of a single axis linear motor test-bed. A simple theoretical model of the system is also presented and the performance of the linear motor driven axis is analysed using both experimental and simulation results. Through further analysis of the linear motor test-bed, the system stiffness and various performance limiting 'disturbance' forces are actually quantified. A similar analysis of a belt driven ball screw axis is then presented, with the results compared.

2 DEVELOPMENT OF THE TEST-BED

As the work undertaken in this project was in conjunction with a manufacturer of laser cutting machine tools, the linear motor test-bed was designed to replicate one axis of a laser cutting machine. The long travels, high speeds and zero machining forces associated with the laser cutting process are commonly thought to be ideal for a linear motor.

The specific design requirements of the linear motor driven axis included a travel of approximately 1.5m, a maximum velocity of at least 2m/s, a maximum acceleration of at least 10m/s^2 (for a 40kg payload) and a

duty cycle of 20%.

The motor selected to meet the test-bed design requirements was a 'tubular' style linear motor from Linear Drives Ltd in the United Kingdom (Model: LD3806). This type of linear motor consists of a thrust block containing three phase armature windings and a tube housing permanent magnets for field excitation (this tube passes through the centre of the thrust block). Through a balancing of the forces, the 'tubular' style linear motor eliminates the magnetic attraction that exists between the separate armature and field components of more common 'flat' style linear motors. This magnetic attraction can often be up to an order of magnitude higher than the actual payload (affecting supporting rail requirements, peak force requirements, cooling and cost), and is a particular problem in high force iron-core motors.

The LD3806 linear motor produces a 750N peak force, a 243N continuous force and has a peak velocity of 4.5m/s [5]. It can be seen that these specifications are sufficient to achieve all of the performance related design requirements.

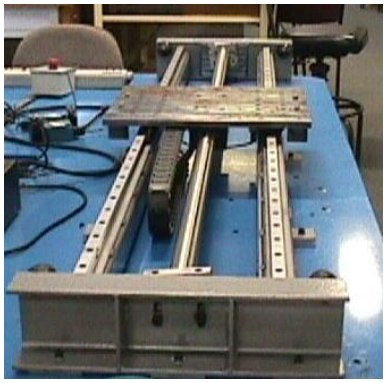

Figure 1: Linear Motor Test-Bed

A photograph of the linear motor test-bed is shown in Figure 1. As can be seen, the basic test-bed structure consists of a simple steel frame carrying two linear rails. The linear rails support a moving table (for mounting various loads). The field excitation rod is mounted in the centre of the test-bed and passes through the thrust block, which is attached to the moving table. The complete test-bed structure is mounted on a separate rigid support table.

A Renishaw ® incremental linear encoder (Model: RGS-S/RGH22B) is mounted on one side of the frame structure. This encoder is used for both position feedback and commutation information. The linear motor test-bed is driven by a complete industry CNC system. This system consists of a servo power supply, two digital servo drives, a SERCOS input/output unit and a safety stop unit, all mounted on a light steel frame. The CNC software is running on a standard Intel Pentium III ® desktop computer. Communication between the digital servo drives, the input/output unit and the PC is handled by SERCOS (SErial Real time COmmunications System). SERCOS is based on the international standard IEC 1491 and exchanges data via a fibre optic ring.

3 MATHEMATICAL MODELLING

3.1 Linear Motor System

3.1.1 Basic Model

For the purposes of simulation and controller design, it is appropriate to develop a mathematical model of the linear motor system. For this reason, a diagram of the basic linear motor test-bed is given in Figure 2, where:

- F_m is the force produced by the linear motor,
- F_d represents general external disturbances,
- B_m is the viscous friction coefficient of the load,
- x is the linear displacement of the load and
- M is the total mass of the load (including the motor thrust block and linear bearings).

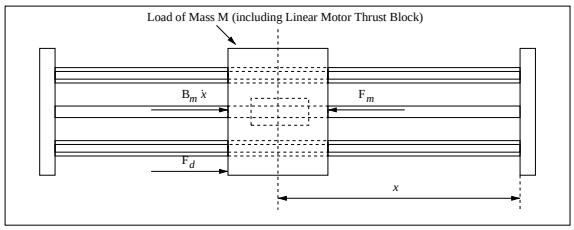

Figure 2: Diagram of Linear Motor Test-Bed

Hence, the equation of motion for the system given in Figure 2 is:

$$M\ddot{x} = F_m - B_m\dot{x} - F_d \tag{1}$$

As can be seen, Equation (1) represents a very basic mathematical model of the linear motor test-bed. The term F_d represents all disturbance forces acting on the system. As some of these forces are not strictly external, such as coulomb friction and periodic cogging forces, a more accurate model would include additional terms representing the inherent system disturbances. However, since all of these factors are seen by the motor as general disturbances, it is fair to treat them this way in a basic model. One of the aims of this paper is to quantify the inherent disturbances that significantly affect system performance. From these results it would be possible to build a more accurate system model.

3.1.2 Dynamic Stiffness

Dynamic stiffness, as a function of frequency, can be determined for the basic linear motor test-bed. Considering a maximum position error (E), resulting from a disturbance force, the position displacement (x) can be described as:

$$x(t) = \mathrm{E}\sin(2\pi f t) \tag{2}$$

Differentiation of Equation (2) leads to the following descriptions of velocity and acceleration:

$$\dot{x}(t) = 2\pi f \mathrm{E}\cos(2\pi f t) \tag{3}$$

$$\ddot{x}(t) = -(2\pi f)^2 \mathrm{E}\sin(2\pi f t) \tag{4}$$

If the system in Equation (1) is uncontrolled ($\mathrm{F_m} = 0$):

$$\begin{aligned}\mathrm{F}_d = &-\mathrm{M}(-(2\pi f)^2 \mathrm{E}\sin(2\pi f t)) \\ &-\mathrm{B}_m(2\pi f \mathrm{E}\cos(2\pi f t))\end{aligned} \tag{5}$$

Hence, assuming a small viscous friction coefficient, the magnitude of the disturbance force is:

$$\mathrm{F}_d \approx \mathrm{M}(2\pi f)^2 \mathrm{E} \tag{6}$$

Since dynamic stiffness is defined as the ratio of an applied force to the system response to that force, the magnitude of dynamic stiffness (DS) is:

$$\mathrm{DS} \approx \mathrm{M}(2\pi f)^2 \tag{7}$$

3.2 Ball Screw System

3.2.1 Basic Model

For comparison purposes, a diagram of a more conventional belt driven ball screw system is shown in Figure 3. The equation of motion for the system given in Figure 3 is:

$$\begin{aligned}&\left[\mathrm{M}_t + \left[\frac{2\pi}{\mathrm{P}}\right]^2 \left[\mathrm{J}_{bs} + \left[\frac{\mathrm{N}_2}{\mathrm{N}_1}\right]^2 \mathrm{J}_m\right]\right]\ddot{x} \\ &= \frac{2\pi}{\mathrm{P}}\left[\frac{\mathrm{N}_2}{\mathrm{N}_1}\left[\mathrm{T}_m - \mathrm{B}_m\dot{\theta}_m - \mathrm{T}_{dism}\right]\right] \\ &\qquad -\frac{2\pi}{\mathrm{P}}\left[\mathrm{B}_{bs}\dot{\theta}_{bs} + \mathrm{T}_{disbs}\right] \\ &\qquad -\mathrm{B}_t\dot{x} - \mathrm{F}_{dis}\end{aligned} \tag{8}$$

where:

- M_t is the mass of the moving table,
- J_m and J_{bs} are the motor and ball screw inertias respectively,
- P is the pitch of the ball screw,
- N_1 and N_2 are the number of teeth on the motor and ball screw pulleys respectively,
- B_t, B_m and B_{bs} are the viscous friction coefficients of the table, motor and ball screw respectively,
- x is the linear displacement of the load,
- θ_m and θ_{bs} are the angular displacements of the motor and ball screw respectively,
- T_m is the motor torque,
- F_{dis} represents disturbance forces at the table and
- T_{dism} and T_{disbs} represent disturbance torques at the motor and ball screw respectively.

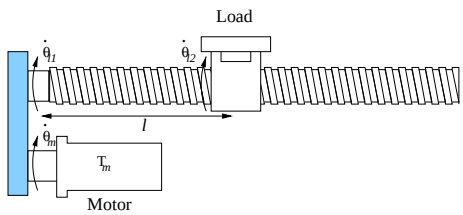

Figure 3: Diagram of a Belt Driven Ball Screw

Again, the model represented by Equation (8) is very basic. For simplicity, backlash and structural flexibility of the ball screw and belt/pulley system have not been included. Although these factors can be minimised through improved mechanical design, they are still present in any ball screw system.

3.2.2 Dynamic Stiffness

Dynamic stiffness can also be determined for the basic ball screw driven test-bed. From equations (2), (3), (4) and (8), if $\mathrm{T}_m = 0$ (an uncontrolled system) and all viscous friction elements and torque disturbances are assumed to be negligible:

$$\begin{aligned}\mathrm{F}_{dis} \approx -&\left[\mathrm{M}_t + \left[\frac{2\pi}{\mathrm{P}}\right]^2 \left[\mathrm{J}_{bs} + \left[\frac{\mathrm{N}_2}{\mathrm{N}_1}\right]^2 \mathrm{J}_m\right]\right] \\ &\times(-(2\pi f)^2 \mathrm{E}\sin(2\pi f t))\end{aligned} \tag{9}$$

and the magnitude of the dynamic stiffness is:

$$\mathrm{DS} \approx \left[\mathrm{M}_t + \left[\frac{2\pi}{\mathrm{P}}\right]^2 \left[\mathrm{J}_{bs} + \left[\frac{\mathrm{N}_2}{\mathrm{N}_1}\right]^2 \mathrm{J}_m\right]\right](2\pi f)^2 \tag{10}$$

In this case it should be noted that motor and ball screw disturbances are not really negligible. In Equations (9) and (10) they have been neglected for simplicity. However, these disturbances are quite large when reflected to the load through the mechanical transmission, resulting in an increase in dynamic stiffness.

4 BASIC POSITIONING OF THE LINEAR MOTOR TEST-BED

Before any testing was performed on the actual linear motor test-bed, the system was simulated using the mathematics package 'Matlab'. With the addition of 'Simulink', a block diagram approach to modelling and simulation was employed. Such simulation is helpful for choosing initial controller gains and predicting system behaviour. A block diagram of the simulation model is shown in Figure 4. The simulated velocity controller consists of proportional and integral terms (with anti-integral windup), while the position controller consists of a simple proportional gain.

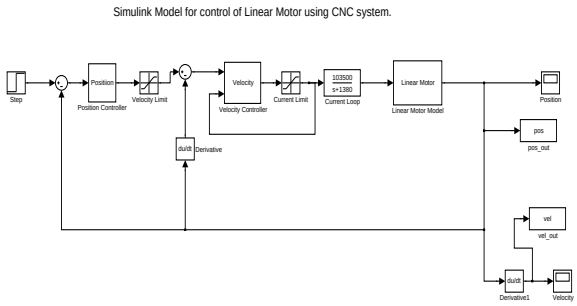

Figure 4: Simulink Model for Linear Motor System

Figure 5 shows the simulated position response of the linear motor system to a step input of 1m and a feedrate of 2.5m/s. As can be seen, the total time taken to move from a standstill to the reference position is approximately 0.65s. The average velocity during this response is approximately 1.5m/s, while the peak velocity is 2.5m/s. Figure 6 shows the response of the actual linear motor test-bed to the same step input.

It can be seen that the response of the simulation model compares quite well with that of the actual test-bed. Both the simulation and real response show a fast smooth transient, with a peak velocity of 2.5m/s. However, there are some differences in the dynamics during acceleration and deceleration, demonstrating the limitations of the current simulation model.

Low speed performance (with feedrates down to 50mm/min) of the linear motor was also analysed, with the system showing a smooth response both in simulation and experimentally.

5 PERFORMANCE COMPARISON

5.1 Stiffness

One important performance limitation of a machine tool positioning axis is dynamic stiffness. Low dynamic

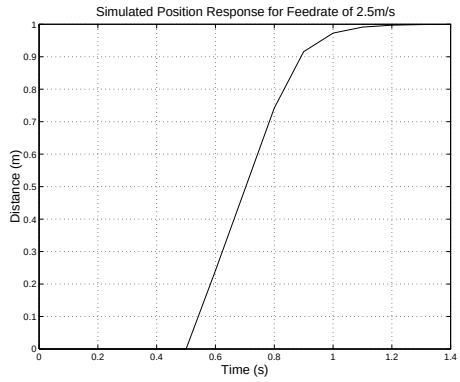

Figure 5: Simulated Position (Feed = 2.5m/s)

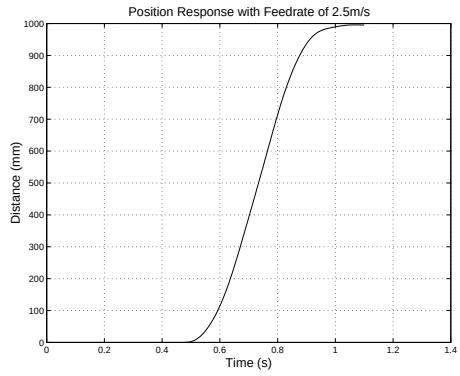

Figure 6: Experimental Position (Feed = 2.5m/s)

stiffness leads to poor disturbance rejection and sensitivity to load variations. Equations (7) and (10) illustrate the inherent dynamic stiffness of a linear motor driven axis and a belt driven ball screw axis respectively. From these equations, it can be shown that the inherent dynamic stiffness of a ball screw driven axis is around 50 times higher than that of a linear motor driven axis (using the same load, along with realistic machine parameters). If all of the friction elements (on both systems) are taken into account, this ratio would increase even further.

To analyse the stiffness of actual test-beds, a 225N disturbance force was suddenly applied to both the linear motor test-bed and a comparable ball screw driven axis in steady-state position control. The position response of the linear motor is shown in Figure 7, while the position response of the ball screw driven axis is shown in Figure 8.

A maximum position error of approximately 1.5mm can be seen in the response of the linear motor. In an actual machine tool, a position error of this magnitude would result in poor surface finish on the work piece and possibly tool damage. As expected, a much smaller position error was seen in the response of the ball screw

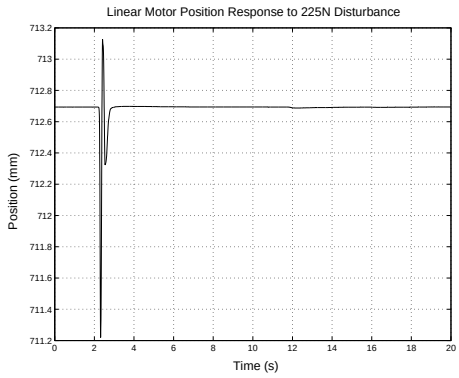

Figure 7: Linear Motor Position (225N Disturbance)

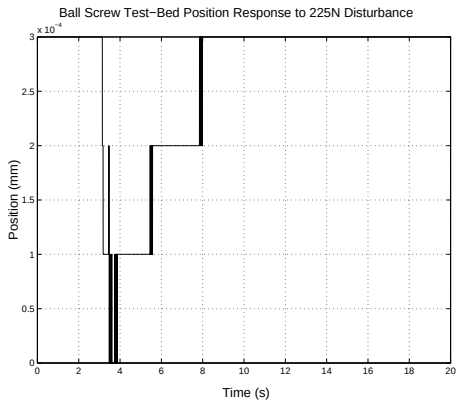

Figure 8: Ball Screw Axis Position (225N Disturbance)

driven axis (0.3 microns). Although the stiffness ratio between the two systems is higher than the theoretical value of 50, it is consistent with the expected increase due to friction terms.

5.2 Position Dependant Torque/Force

5.2.1 Overview

Some of the performance limiting factors on a machine tool axis can be quantified through a study of the periodic torque/force disturbances. It has been shown that useful information about a mechanical system can be obtained by recording drive train torque (or force) as a function of position (not time) [6]. A Fast Fourier Transform (FFT) can be taken for torque/force values recorded at equally spaced position intervals, transforming the signal from the position domain to the "position frequency domain". The resulting "position frequency" spectrum will normally have a relationship to various components in the machine tool drive train.

Consider the system represented by Equation (1). If the system is run at a constant velocity:

$$\mathrm{F}_m = \mathrm{B}_m \dot{x} + \mathrm{F}_d \tag{11}$$

where $\mathrm{B}_m \dot{x}$ is constant.

If coulomb friction is separated from the general term F_d, the resulting motor force (at any position) is equivalent to the constant force required to overcome friction (coulomb + viscous) plus the force required to overcome any disturbances. Hence, the DC component of the FFT is equivalent to coulomb and viscous friction, while the remaining spectrum is associated with the position dependent force variations.

5.2.2 Comparison

The position frequency spectrum of the linear motor test-bed, run at a constant linear velocity of 200mm/min, is shown in Figure 9. The position frequency spectrum of the ball screw driven axis, run at the same constant linear velocity, is shown in Figure 10. It should be noted that the position frequency in these plots has been expressed in cycles per revolution. For the linear motor one revolution is equivalent to one electrical revolution of the motor, while for the ball screw axis one revolution refers to one mechanical revolution of the rotary motor.

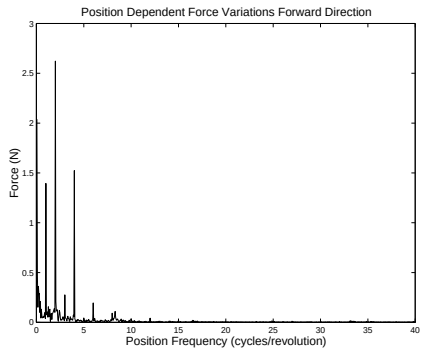

Figure 9: Linear Motor Frequency Spectrum

An analysis of these performance limiting disturbances on the ball screw axis has previously been presented in [7]. However, the results can easily be compared with that of the linear motor test-bed. The DC component (friction) was found to be 18.76N on the linear motor test-bed, compared with a torque of 0.95Nm on the ball screw axis. This equates to 0.0625W of mechanical power supplied by the linear motor to overcome friction, compared with 3.98W by the rotary motor in the ball screw axis. As expected, the power required to overcome friction is much less on the linear motor test-bed, as the only source of friction is the linear support rails.

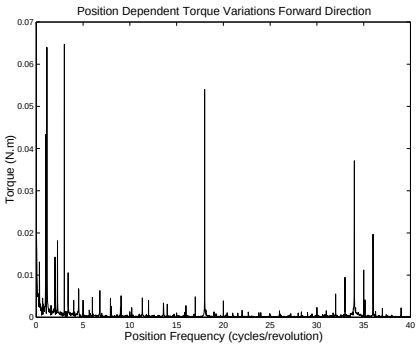

Figure 10: Ball screw Axis Frequency Spectrum

In Figures 9 and 10 the DC component has been set to zero in order to concentrate on other disturbances. In the linear motor spectrum (Figure 9) the largest component was found at 2 cycles/revolution (2.62N), which along with the components at 1 cycle/revolution (1.39N) and 4 cycles/revolution (1.52N) can be attributed to motor cogging forces. The only other significant component is at 0.05 cycles/revolution, which is the fundamental and corresponds to the actual length of travel used in the testing procedure. As such, this component does not relate to a performance limitation.

The frequency spectrum of the ball screw axis (Figure 10) has a larger number of disturbance components. Again a number of components are due to cogging forces in the rotary motor (at 3 and 6 cycles/revolution). However, there are also significant components at 1.14 cycles/revolution (the belt cycle), 1 cycle/revolution (rotor alignment) and at 34 cycles/revolution (the belt pulley cycle). These disturbance components are all significant and are due to the mechanical system. As such, they represent additional performance limitations that are not present on linear motor test-bed.

6 CONCLUSIONS AND FUTURE RESEARCH

The design and development of a linear motor test-bed has been presented in this paper. A simple theoretical model was developed and compared with that of a more conventional belt driven ball screw axis. The basic linear positioning capabilities of the linear motor test-bed were demonstrated both experimentally and through simulation.

A number of performance limiting factors were then quantified and compared between the linear motor test-bed and a belt driven ball screw axis. It was shown that the theoretical dynamic stiffness of a ball screw driven axis was some 50 times higher than that of a comparable linear motor axis. This result was also confirmed experimentally, with the ball screw axis exhibiting even higher stiffness due to friction terms. Through an analysis of position dependent torque/force variations it was shown that the mechanical power required to overcome friction was around 60 times higher on the ball screw axis. Also, as expected, there were a number of mechanical performance disturbances on the ball screw axis that were not present on the linear motor. It was also acknowledged that backlash and structural flexibility would result in further differences between the two systems.

Although the higher attainable speeds and reduced performance limitations of the linear motor system show great advantages, dynamic stiffness is still a concern. Higher dynamic stiffness can only be achieved through improved servo control. However, a reduced number of performance limitations makes higher controller bandwidth possible and this is the focus of current research.

ACKNOWLEDGMENT

Acknowledgment is given for the support provided to this project by the Cooperative Research Centre for Intelligent Manufacturing Systems and Technologies.

REFERENCES

[1] Eric Laithwaite, "Linear electric machines - a personal view," in *Proceedings of the IEEE*, 1975, vol. 63, pp. 250–290.

[2] David Alter and Tsu-Chin Tsao, "Control of linear motors for machine tool feed drives: Experimental investigation of optimal feedforward tracking control," *Journal of Dynamic Systems, Measurement and Control*, vol. 120, pp. 137–142, 1998.

[3] B. Yao and L. Xu, "Adaptive robust control of linear motors for precision manufacturing," in *14th IFAC World Congress*, Beijing, 1999, vol. A, pp. 25–30.

[4] H. Van Brussel and P. Van den Braembussche, "Robust control of feed drives with linear motors," in *CIRP Annals*, Switzerland, 1998, pp. 325–328.

[5] Linear Drives Limited, *Complete Collection of Data Sheets for Linear Drives LD Series Motors*.

[6] B. Armstrong-Hélouvry, *Control of Machines with Friction*, Kluwer Academic Publishers, Massachusetts, USA, 1991.

[7] Simon Webb and Chris Cook, "Identification of drive train torque disturbances for an x-y table test bed," in *Fifth International Conference on Control, Automation, Robotics and Vision*, Singapore, 1998, pp. 439–443.